A review of multiaxial fatigue of weldments: experimental results, design code and critical plane approaches

M. BÄCKSTRÖM and G. MARQUIS

VTT Manufacturing Technology, PO Box 1705, FIN-02044 VTT, Finland

ABSTRACT A survey of biaxial (bending or tension and torsion) constant amplitude fatigue of welded connections is presented. Re-analysis of 233 experimental results from eight different studies has been performed based on hot spot stresses and three potential damage parameters: maximum principal stress range; maximum shear stress range; and a modified critical plane model for welds. Of the three methods, the critical plane model was most successful in resolving the data to a single *S–N* line. The design curve for all toe failures based on the critical plane model was FAT 97 with a slope of 3. By excluding butt welds and including only fillet welds that failed at the weld toe, the design curve was increased to FAT 114 with a slope of 3. However, observed scatter was 70–100% larger than that observed in uniaxial loaded specimens analysed using the hot spot approach.

Keywords biaxial fatigue; multiaxial fatigue; fatigue of welds.

NOMENCLATURE

b = slope of stress–life curve
f = damage function
k = material constant
$K_{s,\sigma}, K_{s,\tau}$ = structural stress concentration factor for normal and shear stress
s = standard deviation in log life
$\Delta\tau'$ = effective shear range
σ_n = normal stress on a plane
σ_n^{max} = maximum value of normal stress on a plane during a load cycle
τ_f^* = constant of critical plane hot spot fatigue strength curve
ϕ, θ = coordinate transformation angles

Subscripts

hs = hot spot stress
nom = nominal stress
x, y, z = specified coordinate system
x', y', z' = transformed coordinate system

INTRODUCTION

Many engineering structures, e.g. vehicle frames and bogies, experience biaxial operational stresses in the vicinity of welded attachments. Principal stress directions may be constant or they may vary during the loading cycle. The former case is normally termed proportional loading, while the latter is non-proportional loading. The Eurocode 3[1] design code recommends that the maximum principal stress range may be used as a fatigue life damage parameter if the loading is proportional. For non-proportional loading, the components of damage for normal and shear stresses are assessed separately using the Palmgren–Miner rule and then combined using an interaction equation. Maximum shear stress range is used as an equivalent stress for non-proportional loading in the ASME code.[2]

Marquis *et al.*[3] proposed a modification to Findley's stress-based model for welded connections. Bäckström *et al.*[4] found that this parameter provided good correlation for proportional and non-proportional fatigue lives of tube-to-plate weldments. Modifications to

Findley's original model were achieved by incorporating hot spot stresses, limiting the orientation of potential failure planes with respect to the weld line, and considering welding residual stresses for non-stress-relieved components.

REVIEW OF MULTIAXIAL FATIGUE DATA FOR WELDED JOINTS

General

Kouba and Stallmayer (1959), Gurney and Woodley (1962), and Braithwaite (1964)[5] were possibly the first researchers to address the question of biaxial fatigue of welded joints. According to Gurney,[5] tests were conducted with proportional loading for beams with fillet stiffeners welded to the web. It was concluded that fatigue lives were better correlated on the basis of maximum principal stress range rather than the uniaxial bending stress range. Archer[6] in 1987 and Siljander *et al.*[7] in 1992 were the first to consider the question of non-proportional loading of welded details. Siljander *et al.* found that non-proportional loading was more damaging than proportional loading, while Archer found them to be equally damaging. An overview of the test series carried out by different researchers during the past 15 years is given in Table 1. While this table lists a total of 314 test data points, only the 233 points that produced weld toe failures are re-analysed here. Weld root/throat failures are excluded from this paper.

Test data

In 1986, Yung and Lawrence[8] performed biaxial fatigue tests on circular tube-to-plate welded specimens [Fig. 1(a)]. The specimens, 14 as-welded and four stress-relieved, were fabricated from ASTM A519 cold-drawn seamless steel tube. These fatigue tests were conducted with bending only, torsion only and proportional bending–torsion loading. Stress ratios, $\sigma_{nom.min}/\sigma_{nom.max}$ and $\tau_{nom.min}/\tau_{nom.max}$, were -1 in all tests. The experimental nominal bending-to-shear stress ratios, $\sigma_{nom.max}/\tau_{nom.max}$, ranged from 1.7 to 2.9 in combined bending–torsion tests. A total of 18 specimens was tested, and fatigue lives ranged from 1×10^4 to 2×10^6 cycles. All specimens failed at the weld toe. Experimental data were correlated using the amplitudes of local bending stress, local octahedral shear stress and local maximum principal stress. The best correlation of the test data was obtained when the shear stresses were included in the analysis.

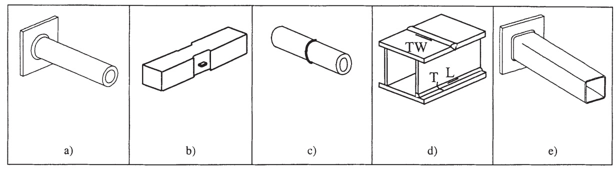

Fig. 1 Specimen geometry of: (a) circular tube-to-plate; (b) box beams with longitudinal attachments; (c) circular tube-to-tube; (d) welded box beam (TW, crack in transverse weld; T, transverse crack; L, longitudinal crack); and (e) rectangular tube to plate.

In 1987, Archer[6] investigated the behaviour of structural box beams with two welded longitudinal attachments. Attachments were fillet welded to the webs of the box beams where the thickness had been reduced [Fig. 1(b)]. Specimens were made of BS 4360 grade 43C steel and tested in the as-welded condition. Loading modes were bending, torsion, and proportional and non-proportional combined bending–torsion. It should be noted that the phase difference in non-proportional tests was produced by using different frequencies for the bend and torsion loads. This leads to a cumulative damage problem, because smaller stress variations will be added to the main cycle. The normal stress ratio was 0 or -1, and the shear stress ratio -1. Reported bending-to-torsion stress ratios ranged

Table 1 An overview of the test series carried out by different researchers with plate thickness from 3 to 10 mm

Test results	Specimen (No.)	Bending or tension only (No.)	Torsion only (No.)	Bending/tension and torsion proportional (No.)	Bending/tension and torsion non-proportional (No.)
Archer[6]	27	1	10	5	11
Yung and Lawrence[8]	18	5	2	11	0
Siljander *et al.*[7]	40	10	10	10	10
Sonsino, tube–tube[9,10]	78	25	8	24	21
Sonsino, tube-to-plate[9,10]	47	7	0	20	20
Razmjoo[11]	29	7	8	7	7
Bäckström *et al.*[4]	22	5	4	9	4
Dahle *et al.*[12]	53	6	22	21	4
Total	314	66	64	107	77

from 0.8 to 2.1 in the combined bending–torsion fatigue tests. A total of 27 specimens were tested. Fatigue lives ranged between 1×10^5 and 4×10^6 cycles, and all specimens failed at the weld toe. Archer found that his fatigue test results were satisfactorily correlated using both an interaction equation approach and a 'maximum damage' computational procedure. This analysis with the available limited experimental data suggested no pronounced difference between proportional and non-proportional loading.

In 1992, Siljander *et al.*[7] reported biaxial fatigue tests for circular tube-to-plate welded joints [Fig. 1(a)], under proportional and non-proportional loading. Stress-relieved specimens were fabricated from ASTM A519 cold-drawn seamless steel tube. Dimensions of Siljander's specimens were nearly identical to those of Yung and Lawrence. A total of 40 fatigue tests, bending only, torsion only and combined bending–torsion, were conducted. Fatigue lives ranged from 1×10^4 to 2×10^6 cycles. The bending stress ratio was 0 or -1, and the nominal bending-to-shear stress ratio was 1–7.4 in combined bending–torsion fatigue tests. All specimens failed at the weld toe. Test results were correlated using various multiaxial fatigue damage parameters based on the local stresses. Local stresses at the weld toe were calculated with the FE-method. They found that the test results for both the proportional and non-proportional load histories were best correlated using Findley's equivalent shear stress model. It was noted that $\sim 80\%$ of the total fatigue life was spent in initiating the fatigue cracks.

Sonsino[9,10] tested 47 circular tube-to-plate [Fig. 1(a)] and 78 tube-to-tube joints [Fig. 1(c)] with unmachined and machined welds. Bending only, torsion only, and proportional and non-proportional combined bending–torsion loading were used in these tests. All tests were conducted at a stress ratio of -1, and the nominal bending-to-torsion ratio was 1.7 in the combined tension–torsion fatigue tests. Specimens were stress relieved and failed at the weld toe. Fatigue lives ranged between 1×10^4 and 4×10^6 cycles. It was found that neither the maximum principal stress criterion nor the von Mises criterion were relevant for non-proportional combined bending–torsion loading. A new hypothesis for welded joints under multiaxial loading based on the effective equivalent stress (EESH) was proposed. This method assumes that cracks initiate by shear, and involves calculating the interaction of all shear stress components in a surface- or volume-element at the weld toe. Stresses are calculated from the local strains and shear stresses at the weld toe.

Razmjoo[11] investigated the fatigue performance of fillet welded tube-to-plate specimen [Fig. 1(a)]. Specimens were in the as-welded condition and tested under tension only, torsion only, and proportional and non-proportional combined tension–torsion loading. All tests were conducted at a stress ratio of zero. The nominal tension-to-shear stress ratio ranged from 0.33 to 2 in the combined tension–torsion fatigue tests. A total of 29 specimens were tested in the range of 1×10^5–1×10^7 cycles to failure. All cracks initiated at the weld toe in the tension only and the combined tension–torsion cases. Most of the specimens tested in torsion cracked at the weld throat. It was found that the maximum principal stress range was a better criterion for proportional loading than the von Mises criterion. In the case of non-proportional loading, neither of the analysis methods was entirely satisfactory. Razmjoo suggested that the maximum principal stress range can be used for non-proportional loading with an extra safety factor of 1.7 when using the design *S–N* curves in BS 5400 or BS 7608.

Dahle *et al.*[12] reported multiaxial fatigue test results on welded box beams [Fig. 1(d)], which were fabricated of Domex 350 and Weldox 900 high-strength steel. A total of 53 tests under bending only, torsion only, and combined proportional and non-proportional bending–torsion loading were performed. Fatigue lives ranged from 1×10^4 to 3×10^6 cycles. Stress ratios were -1 or 0, and the nominal bending-to-shear stress ratio was 0.5–1.7 for combined bending–torsion fatigue. Three different crack systems were found during testing: longitudinal cracks (L); transverse cracks (T); and cracks along the transverse welds (TW). Results were compared using the maximum principal stress and von Mises criteria. It was found that the maximum principal stress criterion was not relevant for proportional or non-proportional combined bending–torsion loading. It can be noted that Dahle *et al.*[12] report both weld root and weld toe failures, but only the weld toe failures are re-analysed here.

Bäckström *et al.*[4] performed bending only, torsion only, and proportional and non-proportional combined bending–torsion fatigue tests. Specimens were square hollow section tube-to-plate joints [Fig. 1(e)] in the as-welded condition. The bending only fatigue tests were conducted using the recommendation of Ohta *et al.*,[13] which uses a different stress ratio for each stress range. In all other tests the stress ratio was -1 or 0. A total of 22 specimens were tested and fatigue lives ranged between 1×10^4 and 2×10^6 cycles. Fatigue cracks initiated at the weld toe during bending only and combined bending–torsion fatigue tests. For torsion only tests, fatigue cracks initiated and grew in the base material near a corner of the tube. The hot spot principal stress range was compared to an approach employing critical plane concepts as the fatigue damage parameter. Both parameters were thickness corrected. It was found that the critical plane model resulted in a better correlation of the data than did the principal stress range.

Structural stress concentration factors

The term 'hot spot' refers to the critical point in a structure where fatigue cracking can be expected to occur due to a discontinuity and/or a notch. Usually the hot spot is located at a weld toe. Hot spot stresses, σ_{hs}, τ_{hs}, are the values of the structural stresses at the hot spot, but exclude the local stress peak produced by the weld toe as illustrated in Fig. 2. The nominal stresses, σ_{nom}, τ_{nom}, are those calculated using simple elasticity formulae found in the literature. The hot spot and nominal stresses are related by structural stress concentration factors for normal and shear stresses:[14]

$$K_{s,\sigma} = \frac{\sigma_{hs}}{\sigma_{nom}}; \qquad K_{s,\tau} = \frac{\tau_{hs}}{\tau_{nom}} \tag{1}$$

Table 2 presents structural stress concentration factors for the five specimens shown in Fig. 1. Lehtonen[15] has calculated the structural stress concentration factors for normal and shear stress for Siljander's version of specimen 1a, and for specimen 1e using solid elements. He has also determined the structural stress concentration factor for normal stress for Sonsino's version of specimen 1a. The normal and shear stress concentration factors for the tube-to-tube specimen, 1c, are expected to be small and are assumed to be unity in this study. Because of the nearly identical geometry, the specimens of Yung and Lawrence are considered to have the same structural stress concentration factors as those of Siljander. Structural stress concentration factors for Razmjoo's version of specimen 1a are estimated from Lehtonen's FE-calculations employing slightly different boundary conditions. The stress concentration factors of Siljander's test specimen were calculated using a non-rigid bolted boundary condition and Razmjoo's with fixed boundary conditions. For Archer's test specimen, 1b, the structural stress concentration factor for normal stress was calculated with a parametric formula.[16] It is not clear if Archer's reported stress values are nominal or include some notch effect. Here it is assumed that the reported stresses are nominal, but if the reported values do include some notch effect, the hot spot stresses may be 10–20% too large. The structural stress concentration factor for shear stress was assumed to be unity in this study.

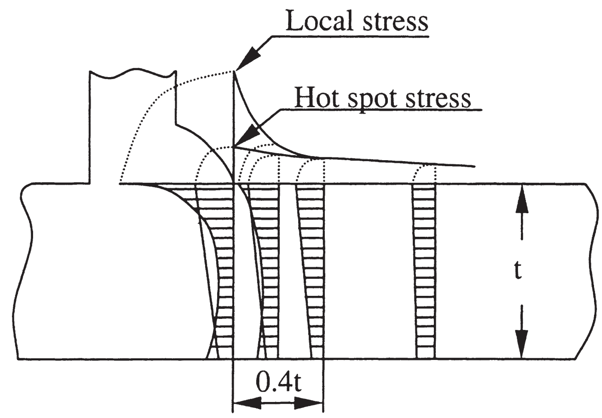

Fig. 2 Stress distributions across the plate thickness and along the surface in the vicinity of a weld toe.

A CRITICAL PLANE APPROACH

Critical plane models have largely developed from observations of fatigue cracking behaviour of smooth specimens which show that cracks initiate and propagate in preferential orientations. Brown and Miller[17] reviewed the available data on multiaxial fatigue and emphasized the importance of the plane orientation for early crack growth. They noted that an appropriate damage model should relate the observed cracking behaviour with strain components acting on the planes of cracking. In contrast to critical plane models are traditional multiaxial fatigue theories that are often extensions of multiaxial yield criteria. These empirical models can be made to fit some of the available data by the inclusion of suitable constants, but are incapable of capturing the complex load interactions often observed in more general multiaxial fatigue loading. One of the first critical plane fatigue damage

Table 2 Structural stress concentration factors

Test specimen	Figure	Thickness (mm)	$K_{s,\sigma}$	$K_{s,\tau}$	Type of weld
Archer[6]	1b	6.0	1.8	1.0	Fillet weld
Yung and Lawrence[8]	1a	8.0	1.25	1.1	Fillet weld
Siljander *et al.*[7]	1a	9.5	1.25	1.1	Fillet weld
Sonsino, tube–tube[9,10]	1c	6.0	1.0	1.0	Butt weld
Sonsino, tube-to-plate[9,10]	1a	10	2.2	1.1	Full penetration fillet
Razmjoo[11]	1a	3.2	1.4	1.1	Fillet weld
Bäckström *et al.*[4]	1e	5.0	3.0	1.3	Full penetration fillet
Dahle *et al.*[12]	1d	8 and 10	1.0	1.0	Butt and Fillet

models was developed by Findley[18] and is based on the alternating shear stress modified by the normal stress on the plane of failure.

Findley suggested that the normal stress, σ_n, on a shear plane had a linear influence on the allowable alternating shear stress, $\Delta\tau/2$.

$$\frac{\Delta\tau}{2} + k\sigma_n = \frac{\Delta\tau'}{2} = f \tag{2}$$

Any combination of $\Delta\tau$ and σ_n resulting in the same effective shear range, $\Delta\tau'$, gives the same fatigue life. The constant k represents a material's sensitivity to normal stress on a shear plane. Failure is expected to occur on the plane that has the largest $\Delta\tau'$, and not necessarily the plane of largest alternating shear stress. Often the superscript 'max' is added to represent the maximum value of normal stress that occurs during a load cycle, σ_n^{max}.

Five modifications of the original Findley model were suggested by Marquis *et al.*[3] to make it more suitable for welded structures.

1 In welded constructions, the vast majority of cracks are initiated along the weld toes where regions of high stress concentration and local geometric irregularities exist. Therefore, the critical damage plane is assumed to be a shear plane parallel to the line of the weld toe. Other planes are neglected.
2 Maximum normal stresses on a damage plane are computed by assuming yield strength magnitude stresses normal to the weld toe or, in the case of stress-relieved joints, the maximum applied hot spot normal stress during the load spectrum. If the maximum applied stresses cause yielding at the hot spot, the maximum normal stress on the damage plane is computed based on the yield strength.
3 The hot spot technique documented by Niemi[14] is used to estimate the local normal stress along the weld toe. Either strain gauges or FEM analysis can be used to determine the normal hot spot stress concentration factors.
4 Stress gradients for shear are highly localized and cannot be effectively measured using strain gauge techniques. Hot spot stress estimates based on FEM are used for determining the shear stress along the weld toe.
5 The damage function, f, in Eq. (2) is assumed to be linear in a $\log(N_f)$ versus $\log(\Delta\tau')$ plot.

$$\Delta\tau'_{hs} = \Delta\tau_{hs} + 2 \cdot k \cdot \sigma_{n,hs}^{max} = \tau_f^*(N_f)^b \tag{3}$$

where τ_{hs} is the hot spot shear stress and $\sigma_{n.hs}^{max}$ is maximum of either the yield strength of the material or, for stress-relieved joints, the largest applied hot spot stress occurring during one application of the load cycle.

The first modification to the critical plane model for welds can be illustrated by considering the tube-to-plate weld shown in Fig. 3 which is subject to bending and torsion loads as shown. The line of the weld toe in the region of highest stress is parallel to the y-axis, and therefore the possible critical planes are limited to those being perpendicular to the x–z plane, i.e. $\theta = 0°$ as defined in Fig. 3.

Also shown in this figure are the proposed potential critical planes. These comprise any plane orientated at

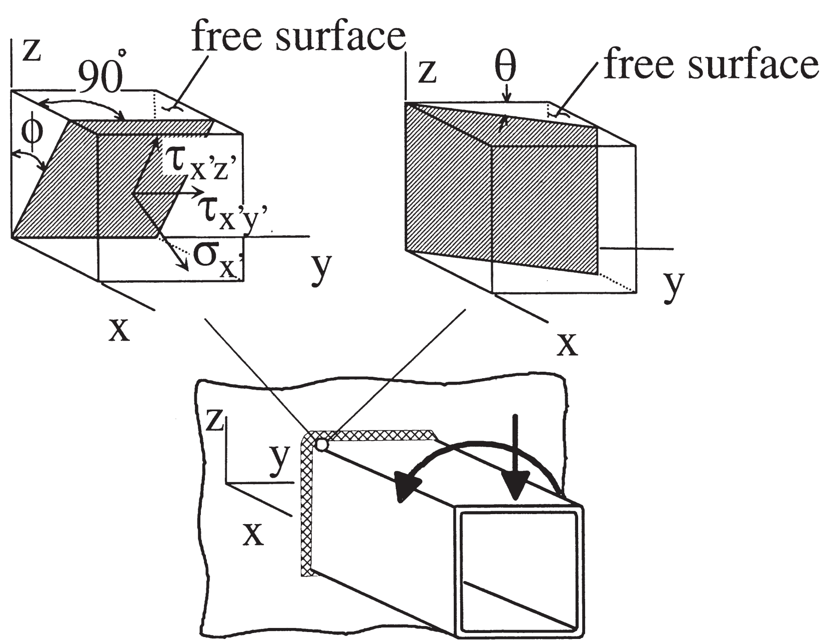

Fig. 3 Damage plane orientation at the weld toe.

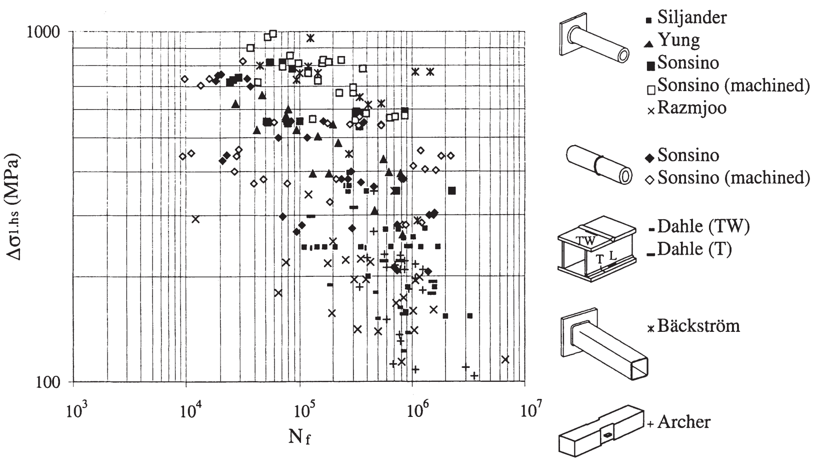

Fig. 4 Fatigue test results for welded joints under multiaxial loading using the maximum hot spot principal stress range approach.

an angle ϕ with respect to the y–z plane. For each load history, suitable coordinate transformation relations can be used to find the angle ϕ that represents the largest combination $\Delta\tau/2 + k\sigma_n^{max}$ during one cycle or, for more complex histories, during one repetition of the load history. Fatigue life for the component is computed using Eq. (3) for the plane of maximum damage. Different angles ϕ will be computed depending on the ratio of bending to torsion and the phase relationship. For complex multiaxial load histories, locating the plane experiencing maximum damage requires a search routine as it may change from cycle to cycle. However, it is usually sufficient to calculate damage on planes at 10° intervals because the damage on planes orientated $\pm 5°$ from the critical plane will show virtually the same value of the damage parameter.

If the only two applied loads are σ_x due to bending and τ_{xy} due to torsion loads, it can be shown using appropriate coordinate transformation relations that the normal stress and shear stresses acting on a plane orientated ϕ are given as

$$\begin{aligned} \sigma_{x'} &= \sigma_x \cos^2 \phi \\ \tau_{x'y'} &= \tau_{xy} \cos \phi \qquad (4) \\ \tau_{x'z'} &= -\sigma_x \cos \phi \sin \phi \end{aligned}$$

From these, the stress state on any plane can be computed throughout the load history.

RESULTS

Maximum principal stress approach

In Eurocode 3,[1] the application of maximum principal stress range for welded structures is recommended when the combined effect of bending and shear must be considered. Figure 4 shows the relationship between fatigue life of welded joints and maximum hot spot principal stress range. A total of 233 test results with weld toe failure under bending, torsion, and proportional and non-proportional combined bending–torsion loading were obtained from Refs [4,6–12].

It should be noted that the assessment of maximum principal stress range is limited only to proportional loading cases in the design code. However, non-proportional fatigue test results are included in the analysis here. Maximum principal stress range is determined from the maximum changes in the stress components during the loading event.[19] This means that the principal stress range is determined at each point in time during the cycle from the changes in stress component. For comparison of the effect of proportional and non-proportional loading, Sonsino's and Siljander's fatigue test results are shown in Fig. 5.

Maximum shear stress range

Maximum shear stress range is used as the damage parameter by ASME[2] when the directions of the principal stresses change during the stress cycle. Maximum shear stress range is determined as the greatest algebraic difference between principal stresses during the whole loading event. Principal stresses are determined at each point in time during the cycle from the changes in the individual normal and shear stress components. This method may be used for welded structures if the principal planes are less than 45° apart, but may be too conservative for greater angles.[19] It should be noted that the ASME code method is not applied directly here as it requires knowledge of the local stresses, while this paper uses hot spot stresses. Test data for all specimens are plotted in terms of maximum hot spot shear stress range in Fig. 6, and a smaller set of tube-to-plate specimen data is shown in Fig. 7.

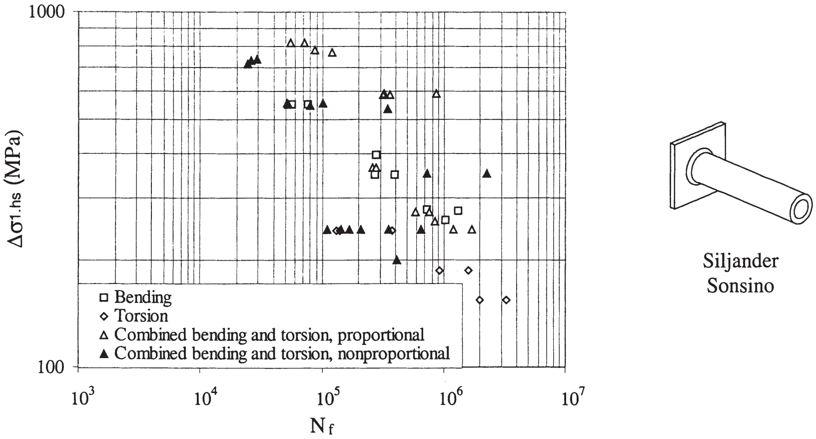

Fig. 5 Fatigue test results for tube-to-plate welded joints under proportional (bending, torsion, and combined bending and torsion) and non-proportional (combined bending and torsion) loading using the maximum hot spot principal stress range approach.

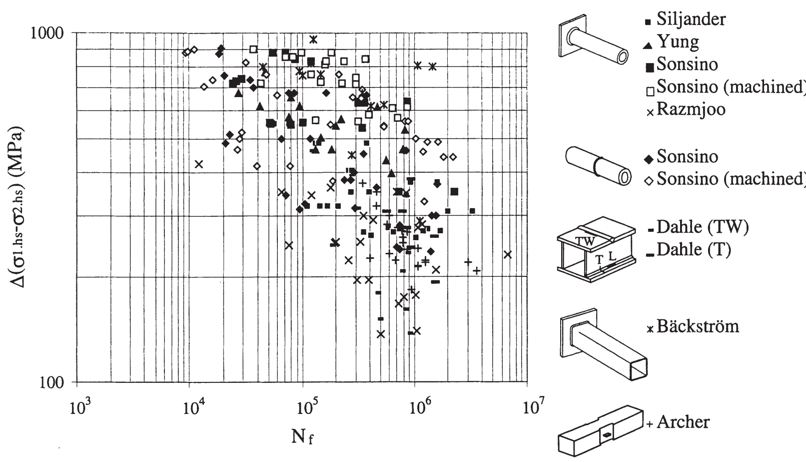

Fig. 6 Fatigue test results for welded joints under multiaxial loading using the maximum hot spot shear stress range approach.

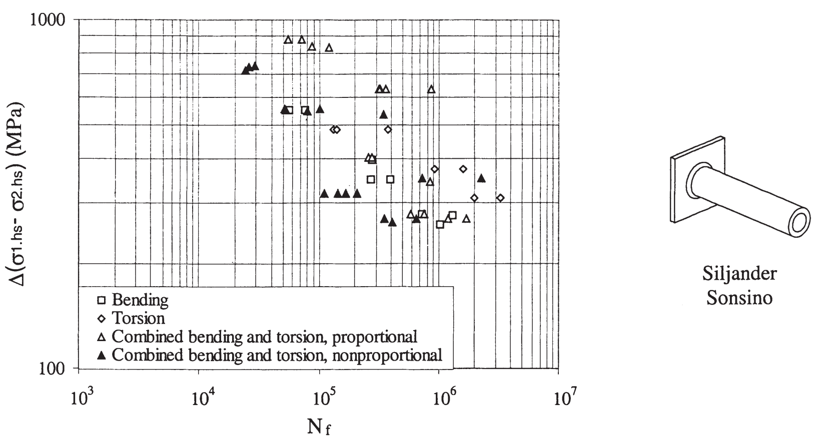

Fig. 7 Fatigue test results for tube-to-plate welded joints under proportional (bending, torsion, and combined bending and torsion) and non-proportional (combined bending and torsion) loading using the maximum hot spot shear stress range approach.

Modified critical plane model for welds

Test data for welded joints were also analysed using the critical plane approach described earlier. In the calculations, Findley's material constant k was assumed to be 0.3 which is a typical value for structural steel.[18] Figure 8 shows the relationship between fatigue life of welded joints and maximum hot spot effective shear range. The effect of proportional and non-proportional loading is illustrated by the smaller data set shown in Fig. 9.

Evaluation of scatter

Scatter in Figs 4–9 was analysed using linear regression by assuming *S–N* slopes of both 3 and 5 according to the method proposed by Hobbacher.[20] Table 3 summar-

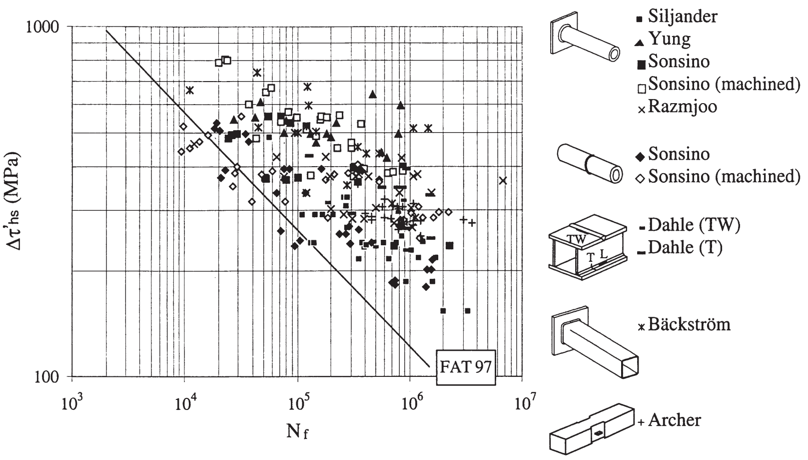

Fig. 8 Fatigue test results for welded joints under multiaxial loading using the hot spot critical plane approach.

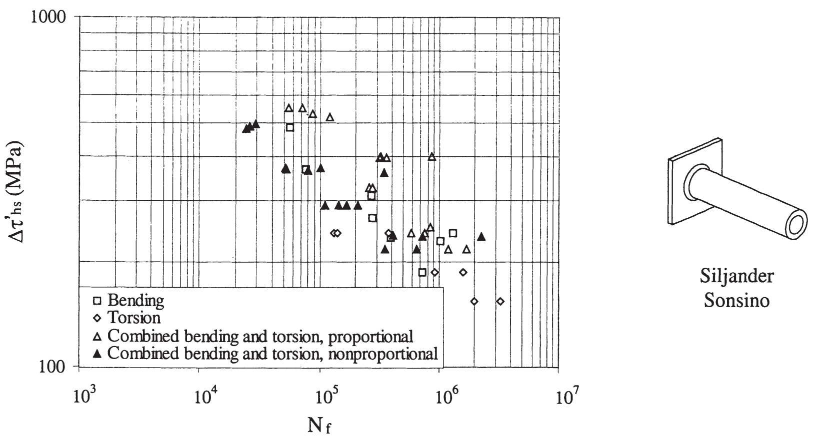

Fig. 9 Fatigue test results for tube-to-plate welded joints under proportional (bending, torsion, and combined bending and torsion) and non-proportional (combined bending and torsion) loading using the hot spot critical plane approach.

izes the analyses and shows the standard deviation in $\log(C)$, s, for each of the three analysis methods and two slopes. The upper part of the table shows all 233 data points representing weld toe failures, while the lower part shows only the 49 circular tube-to-plate joints. As can be seen, the best correlation was obtained using the critical plane approach. The best fit design curve for all 233 data points was FAT 97 with a slope of 3. This design line including all data based on the critical plane model is shown in Fig. 8. The hot spot shear stress range approach was better than the maximum principal stress range approach.

DISCUSSION

Emphasis in the current study is given to hot spot stress-based analyses instead of nominal or local stress-based analyses. It has been reported that nominal stresses do not correlate fatigue strength for multiaxially loaded welds as well as do local stress approaches.[7,9] Nominal stress ranges were reported for all fatigue tests which were found in the literature survey, but weld geometry, e.g. reinforcement angle and toe radius, were not reported in all cases. Parametric formulae for hot spot stress[16] and local stress[21] concentration factors for welded joints can be found in the literature, but local stress concentration factors require knowledge of the local weld geometry making the hot spot stress approach the only means for comparison. Also, during design, hot spot values do not require as detailed a stress analysis, and are therefore more easily applied during the engineering stage of a structure. This is reflected in the newest recommendations for welded joints[1,21] which now allow the use of the hot spot stresses. The hot spot stress

Table 3 Analysis of data scatter for different methods

Test series	Approach	s based on slope 3	s based on slope 5
All test data	$\Delta\sigma_{1.hs}$	0.61	1.02
(233 specimens)	$\Delta(\sigma_{1.hs} - \sigma_{2.hs})$	0.54	0.86
	$\Delta\tau'_{hs}$	0.47	0.58
Sonsino and Siljander	$\Delta\sigma_{1.hs}$	0.46	0.78
(49 specimens)	$\Delta(\sigma_{1.hs} - \sigma_{2.hs})$	0.41	0.60
	$\Delta\tau'_{hs}$	0.33	0.45

approach has been shown to be an effective tool in the case of uniaxial loading and is also worth considering for multiaxial loading.

As seen from Figs 4, 6 and 8, the tube–tube test results tended to have the shortest fatigue life for a given stress parameter, while the rectangular hollow section tests tended to have the longest fatigue lives. For the rectangular hollow section-to-plate welds, the hot spot stress distribution at the corner consisted of two components: membrane stress and shell bending stress. Membrane stress is the average stress through the plate thickness, while shell bending stress is half of the difference between the stress values at the top and bottom surface. The hot spot stress was calculated by multiplying the nominal stress value with the stress concentration factor (SCF) obtained with FE calculations. The SCF does not consider stress gradients and does not differentiate between membrane and bending stress. During the total life of welded components with the same SCF, fatigue cracks grow faster in specimens with greater membrane stress than in specimens with greater shell bending stress. This may be one reason why the computed stress values for the rectangular hollow section specimen are overly conservative. Also, the region of high stress concentration is very small near the square hollow section corner and cracks quickly grow away from this highly stressed region. The small region also means that there is a lesser chance of having a significant defect.

It is interesting to note that Razmjoo's test results were toward the upper end of the scatter band when analysed using the critical plane method (Fig. 8), but toward the lower end of the scatter band when the maximum principal stress and maximum shear stress approaches were used (Figs 4 and 6). These specimens were of higher yield strength steel, and this indicates that the assumption of how residual stresses act on the critical plane may need to be modified for non-stress-relieved joints. Razmjoo's test specimens were loaded with axial tension as compared to the other test series with bending loading. Under axial tension, a greater area of weld is subject to high stress as compared to bending. This means that welding flaws, e.g. weld start/stop, porosity, slag inclusion, lack of fusion or incomplete weld root penetration are more likely to be in a highly stressed region during axial tension. Such flaws provide additional stress concentration which may lead to a reduction in fatigue life. Also the plate thickness of Razmjoo's test specimen was reduced from 7 to 3 mm at the ends of the tube. This may produce additional bending stresses at the weld toe due to eccentricity. Possible bending stresses were not considered in the current analysis.

The effect of proportional and non-proportional loading is seen in Figs 5, 7 and 9 which consider only a subset of the data. These figures show only the circular tube-to-plate specimens tested by Siljander *et al.*[7] and Sonsino.[9,10] Results for proportional and non-proportional loading correlate better for the lower stress levels than at the higher stresses. When data were analysed using the maximum principal stress method (Fig. 5), non-proportional loading was clearly more damaging than proportional loading. This confirms that the maximum principal stress range may not be used for non-proportional loading. The maximum shear stress method (Fig. 7) accounted slightly better for the non-proportional loading, but did not unify the bending only and torsion only data into a single line. The critical plane approach (Fig. 9) did the best job of unifying the four loading modes to a single stress versus life line. However, non-proportional loading still tended to be more damaging and further work on the method is needed.

Scatter in the test results was significant regardless of the analysis method used. In many cases the structural stress at the weld toe may be different from the hot spot stress assumed in the analysis. The tube–tube test results tended to have the shortest fatigue life for a given stress parameter. The apparent short fatigue life for these specimens may be partly explained by the low stress concentration factor, $K_s = 1$, assumed in the analysis. Butt welds, e.g. the tube to tube joint, may also have small offset or angular misalignments which can increase the hot spot stress. Hobbacher[20] observes that misalignment stresses are automatically included if strain gauge techniques are used to determine hot spot stresses, but should also be taken into consideration when using numerical procedures. He also notes that butt welds may have greater or lesser fatigue strength as compared to fillet welds depending on the shape of the weld toe.

Because of this added uncertainty in evaluating the butt welds, Fig. 10 shows only the 163 fillet weld specimens where failure occurred at the weld toe. As in Fig. 8, the critical plane method is used assuming a damage slope of 3. The standard deviation in $\log(C)$ is reduced from $s = 0.47$ based on all data to $s = 0.41$ based on the fillet weld data. The computed design line increases from FAT 97 to FAT 114. For comparison, hot spot stress versus life data for ~ 100 axially loaded specimens have been reported by Partanen and Niemi.[22] The standard deviation in $\log(C)$ was 0.24, i.e. ~ 50–60% of what is observed here for multiaxial loaded welds.

Some of the scatter seen here is probably a result of differences in defining fatigue failure. The precise failure criterion was not reported in most of the studies reviewed, but it was considered to be the final breakthrough or collapse of the test component. Some studies additionally published the life to crack initiation, e.g. life to 1-mm crack depth. Crack initiation life could not be

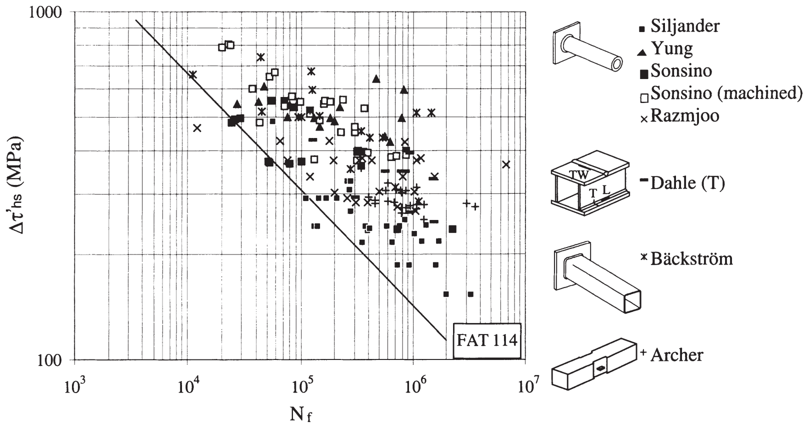

Fig. 10 Fatigue test results for fillet welded joints under multiaxial loading using the hot spot critical plane approach.

used because it was not available for most of the test pieces even though the critical plane model would be expected to correlate initiation life better than final fracture. Studies of non-welded fatigue specimens clearly show that crack growth mode changes as the fatigue process progresses.[23] Maximum shear stress and shear-based critical plane models are more suitable for modelling the growth of short cracks or cracks subject to mode II/III loading, while long cracks subject to mode I loading tend to grow along maximum principal stress planes. A single damage model is expected to be successful for complex loading only if it models the fatigue process that dominates fatigue life.

Further work is required particularly with respect to the effect of residual stresses. This could, in part, be achieved using recently reported uniaxial data where weld geometry and residual stresses have been carefully measured.[24]

CONCLUSIONS

The majority of biaxial fatigue data for welded joints has focused primarily on proportional loading. A total of only 77 non-proportional data points for seven specimen geometries have been reported. The current paper examines 233 experimental results that produced weld toe failure from eight different studies. These have been analysed using three different methods. The three methods are based on hot spot stresses and the maximum principal stress range, maximum shear stress range, and a critical plane model. Hot spot stresses were determined by multiplying nominal stress values published in the literature with a stress concentration factor. Some of the hot spot stress concentration factors were known from FE-analysis, while others were estimated or based on parametric formulae.

Of the three analysis methods, the critical plane model was most successful in resolving the data to a single *S–N* line. The design curve for all toe failures based on the critical plane model was FAT 97 with a slope of 3. By excluding butt welds and including only fillet welds that failed at the weld toe, the design curve was increased to FAT 114 with a slope of 3. However, observed scatter was 70–100% larger than that observed in uniaxial loaded specimens analysed using the hot spot approach. Scatter can be attributed to differences in specimen geometries, test methods, plate thicknesses and the definition of failure.

The maximum principal stress range and the maximum shear stress range could not explain the increased damage normally observed during non-proportional loading as compared to proportional loading. Even the critical plane model needs improvement in explaining the increased damage. The method of accounting for residual stresses and the definition of possible damage planes also requires further work.

Acknowledgements

This study was supported by a grant from The National Technology Agency of Finland (TEKES), Tamrock Corporation, Patria Vehicles and Valmet Automotive Inc.

REFERENCES

1 ENV 1993-1-1 (1992) Eurocode 3: Design of Steel Structures—Part 1-1: General Rules and Rules for Buildings.
2 ASME (1989) ASME Boiler and Pressure Vessel Code. Section III, Rules for Construction of Nuclear Power Plant Components, ASME, New York, USA. Division 1—Subsection NB, Class 1 components.
3 G. Marquis, M. Bäckström and A. Siljander (1997) Multiaxial fatigue damage parameters for welded joints: design code and critical plane approaches. In: *Welded High-Strength Steel Structures* (Edited by A. F. Blom), EMAS, London, pp. 127–141.
4 M. Bäckström, A. Siljander, R. Kuitunen and R. Ilvonen (1997) Multiaxial fatigue experiments of square hollow section tube-to-plate welded joints. In: *Welded High-Strength Steel Structures* (Edited by A. F. Blom), EMAS, London, pp. 163–177.

5 T. R. Gurney (1979) *Fatigue of Welded Structures*, 2nd edition, Cambridge University Press, UK.
6 R. Archer (1987) Fatigue of welded steel attachments under combined direct stress and shear stress. Paper no. 50, *International Conference on Fatigue of Welded Constructions*, 7–9 April 1987, Brighton, UK, The Welding Institute.
7 A. Siljander, P. Kurath and F. V. Lawrence (1992) Nonproportional fatigue of welded structures. In: *Advances in Fatigue Lifetime Predictive Techniques*, *ASTM STP 1122* (Edited by M. R. Mitchell and R. W. Landgraf), ASTM, Philadelphia, pp. 319–338.
8 J.-Y. Yung and F. V. Lawrence (1986) Predicting the fatigue life of welds under combined bending and torsion. UILU-ENG 86–3602, Report no. 125, University of Illinois at Urbana-Champaign, Urbana-Champaign.
9 C. M. Sonsino (1997) Schwingfestigkeit von geschweißten komponenten unter komplexen elasto-plastischen, mehrachsigen verformungen. Fraunhofer Institut Betriebsfestigkeit, Darmstadt. LBF-Nr. 6078. Published by the Commission of European Communities, Luxembourg. EUR-report no. 16024.
10 C. M. Sonsino (1995) Multiaxial fatigue of welded joints under in-phase and out-of-phase local strains and stresses. *Int. J. Fatigue* **17,** 55–70.
11 G. R. Razmjoo (1996) Fatigue of load-carrying fillet welded joints under multiaxial loading, TWI, Abington Cambridge, TWI Ref. 7309.02/96/909.
12 T. Dahle, K.-E. Olsson and B. Jonsson (1997) High strength welded box beams subjected to torsion and bending—test results and proposed design criteria for torsion/bending interaction. In: *Welded High-Strength Steel Structures* (Edited by A. F. Blom), EMAS, London, pp. 143–161.
13 A. Ohta, K. Matsuoka, N. Suzuki and Y. Maeda (1994) Fatigue strength of non-load-carrying cruciform welded joints by a test maintaining maximum stress at yield strength. *Engng Fracture Mech.* **49,** 639–645.
14 E. Niemi (1995) *Stress Determination for Fatigue Analysis of Welded Components*, Abington Publishing, Abington, UK, IIW Doc IIS/IIW-1221-93.
15 M. Lehtonen (1997) On the evaluation of the hot spot stresses using FEM. In: *Welded High-Strength Steel Structures* (Edited by A. F. Blom), EMAS, London, pp. 225–239.
16 E. Niemi, J. Kilkki, I. Poutiainen and V.-M. Lihavainen (1998) *Fatigue Free Design of Welded Joints*, LUT, Lappeenranta, Finland (in Finnish).
17 M. W. Brown and K. J. Miller (1973) A theory for fatigue failure under multiaxial stress–strain conditions. *Proc. Instn. Mech. Engrs* **187,** 745–756.
18 W. N. Findley (1959) A theory for the effect of mean stress on fatigue of metals under combined torsion and axial load or bending. *Trans. ASME, J. Engng Industry* **81,** 301–306.
19 S. J. Maddox (1991) *Fatigue Strength of Welded Structures*, Abington Publishing, Cambridge.
20 A. Hobbacher (1996) Recommendations for fatigue design of welded joints and components. ISO Standard Proposal, IIW Document XIII-1539-96 / XV-845-96, IIW, Paris.
21 K. Iida and T. Uemura (1996) Stress concentration factor formulae widely used in Japan. *Fatigue Fract. Engng Mater. Struct.* **19,** 779–786.
22 T. Partanen and E. Niemi (1996) Hot spot stress approach to fatigue strength analysis of welded components: fatigue test data for steel plate thicknesses up to 10 mm. *Fatigue Fract. Engng Mater. Struct.* **19,** 709–722.
23 D. F. Socie (1993) Critical plane approaches for multiaxial fatigue damage assessment. In: *Advances in Multiaxial Fatigue*, *ASTM STP 1191* (Edited by D. L. McDowell and R. Ellis), ASTM, Philadelphia, pp. 7–36.
24 L. Lopez Martinez, R. Lin Peng, A. F. Blom and D. Q. Wang (1999) Welded and TIG-dressing induced residual stresses—relaxation and influence on fatigue strength of spectrum loaded weldments. In: *Fatigue Design and Reliability*, *ESIS 23* (Edited by G. Marquis and J. Solin), Elsevier Science, Amsterdam, pp. 117–133.

APPENDIX

Example calculation for the critical plane approach

Assume that the tube-to-plate test specimen shown in Fig. 3 is subjected to proportional constant amplitude bending and torsion loading. The nominal normal stress range at the weld toe is $\Delta\sigma_{\mathrm{nom}} = 100$ MPa with a nominal normal stress ratio of $R\sigma = 0$ and the nominal shear stress range at the weld toe is $\Delta\tau_{\mathrm{nom}} = 60$ MPa with a

Table A1 Resultant hot-spot shear stresses ($\tau_{\mathrm{hs},\psi}$) on different planes (ϕ) and directions (ψ)

Time history	$\psi\backslash\phi$	−45°	−30°	−15°	0°	15°	30°	45°
Point 1	0	27.6	33.8	37.7	39.0	37.7	33.8	27.6
	15	65.5	66.2	55.8	37.7	17.0	−1.0	−12.2
	30	98.9	94.2	70.1	33.8	−4.9	−35.7	−51.1
	45	125.6	115.7	79.7	27.6	−26.4	−68.0	−86.6
	60	143.7	129.4	83.8	19.5	−46.1	−95.6	−116.1
	75	152.0	134.2	82.2	10.1	−62.7	−116.7	−137.8
	90	150.0	129.9	75.0	0.0	−75.0	−129.9	−150.0
Point 2	0	−27.6	−33.8	−37.7	−39.0	−37.7	−33.8	−27.6
	15	−26.6	−32.6	−36.4	−37.7	−36.4	−32.6	−26.6
	30	−23.9	−29.3	−32.6	−33.8	−32.6	−29.3	−23.9
	45	−19.5	−23.9	−26.6	−27.6	−26.6	−23.9	−19.5
	60	−13.8	−16.9	−18.8	−19.5	−18.8	−16.9	−13.8
	75	−7.1	−8.7	−9.8	−10.1	−9.8	−8.7	−7.1
	90	0.0	0.0	0.0	0.0	0.0	0.0	0.0

nominal shear stress ratio of $R\tau = -1$. This loading is illustrated in Fig. A1a. Structural stress concentration factors are assumed to be $K_{s,\sigma} = 3$ for normal stress and $K_{s,\sigma} = 1.3$ for shear stress. The assumed stress history of the hot-spot is obtained simply by multiplying the nominal stress by the structural stress concentration factors with the result shown in Fig. A1b. The tube-to-plate specimen is tested as-welded and the yield strength of the tube is $\sigma_y = 355$ MPa and the normal stress sensitivity factor is assumed to be $k = 0.3$.

Hot-spot stresses at points in time and on different planes are easily computed using the equilibrium equations [Eq. (4)]. Because the loading in this example is proportional and constant amplitude, it is sufficient to calculate stresses for two points in the time history. These are indicated as Point 1 and Point 2 in Fig. A1b. With reference to Fig 3, potential critical planes are assumed to be $\theta = 0°$ with angle ϕ varying from $-45°$ to $45°$. Damage varies slowly from plane to plane so in this case damage was computed for planes at 15° intervals. From Eq. (4), two shear stresses on the plane are calculated, $\tau_{x'y'}$ and $\tau_{x'z'}$. These two vector quantities combine to produce a resultant shear stress on the plane. Both the direction and magnitude of this resultant shear change with time. An angle ψ is introduced to indicate the direction of shear (see Fig. A2). The magnitude of shear stress corresponding to $\psi = 0°$ to $90°$ is then computed at both points in time.

For non-stress relieved structures, the normal stress on a plane is derived for the maximum of the σ_y or the maximum applied hot-spot stress. In this example, the $\sigma_y = 355$ MPa while the maximum hot-spot stress during a cycle is only 300 MPa. Table A1 shows the hot-spot shear stress on different planes (ϕ) and in different directions (ψ) at the two points in time. Table A2 presents the hot-spot shear stress ranges determined from Table A1, the maximum hot-spot normal stress [Eq. (4)] and effective hot-spot shear stress range [Eq. (3)] resolved on to various planes (ϕ). For $k = 0.3$, the largest value of the damage parameter, $\Delta\tau'_{hs} =$ 306 MPa, is found to occur on the plane $\phi = -30°$ with the shear direction $\psi = 60°$. The same maximum damage $\Delta\tau'_{hs}$ can be found on other planes, e.g. varying angle ψ from $-90°$ to $0°$. It can be noted that on the $\phi = -30°$ plane, the maximum shear stress at Point 1 is in the direction $\psi = 75°$ and the minimum shear stress at Point 2 is in the direction $\psi = 0°$. However, the maximum range during the entire load cycle is in the direction $\psi = 60°$. It can also be noted that the maximum value of $\Delta\tau'_{hs}$ does not occur on the plane of maximum shear stress nor on the plane of maximum normal stress.

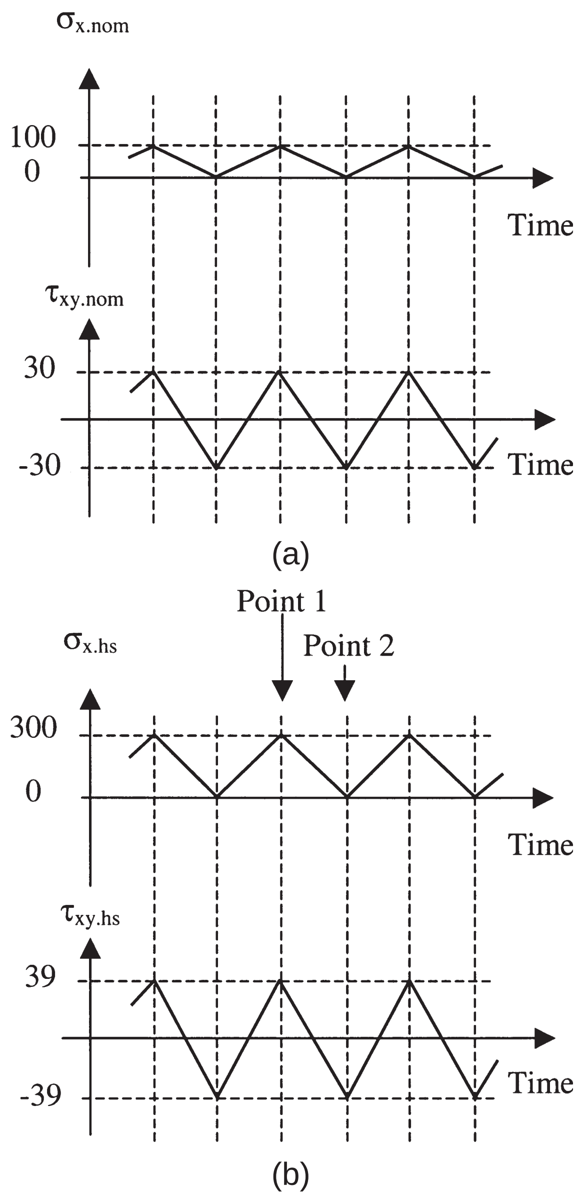

Fig. A1 Normal and shear stress histories for a tube-to-plate test specimen. (a) Nominal values and (b) hot-spot values at the weld toe.

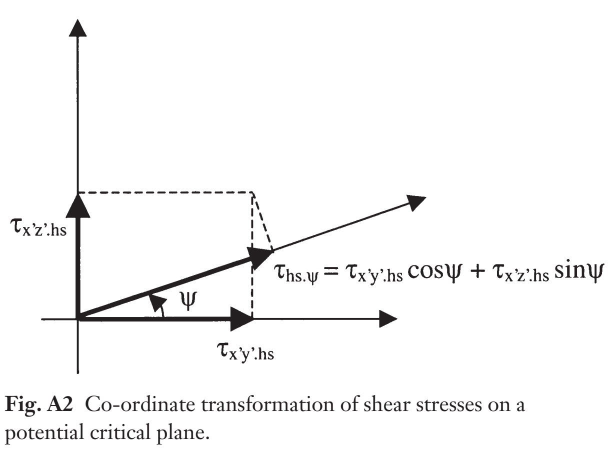

Fig. A2 Co-ordinate transformation of shear stresses on a potential critical plane.

Table A2 Alternating hot-spot shear stress, maximum hot-spot normal stress and effective hot-spot shear stress range on different planes and directions during the load cycle

	$\Delta\tau_{hs,\psi} = \tau_{hs,\psi}^{Point\,1} - \tau_{hs,\psi}^{Point\,2}$						
$\psi\backslash\phi$	$-45°$	$-\mathbf{30}°$	$-15°$	$0°$	$15°$	$30°$	$45°$
0	55.2	67.5	75.3	78.0	75.3	67.5	55.2
15	92.1	98.9	92.2	75.3	53.4	31.6	14.5
30	122.8	123.5	102.7	67.5	27.7	6.5	27.2
45	145.1	139.6	106.3	55.2	0.2	44.1	67.1
60	157.5	**146.3**	102.6	39.0	27.3	78.7	102.3
75	159.2	143.0	91.9	20.2	52.9	108.0	130.6
90	150.0	129.9	75.0	0.0	75.0	129.9	150.0
$\sigma_{n,hs}^{max}$	177.5	**266.3**	331.2	355.0	331.2	266.3	177.5
$\Delta\tau'_{hs}$	265.7	**306.0**	305.0	291.0	274.0	289.7	256.5

The design curve for fillet welds based on the critical plane model and hot-spot stresses is FAT 114 with a slope of 3 (see Fig. 10). Thus, the material constant for critical plane hot-spot strength curve in Eq. (3) is

$$\tau_f^* = (114^3 \cdot 2 \cdot 10^6)^{1/3} = 14363 \quad \text{(A1)}$$

with a slope of $b = -1/3$.

The fatigue life for the test specimen can be calculated from Eq. (3) and Table A2:

$$N_f = \left(\frac{\Delta\tau'_{hs}}{\tau'_f}\right)^{1/b} = \left(\frac{306}{14363}\right)^{-3} = 103000 \text{ cycles} \quad \text{(A2)}$$

This example deals with proportional constant amplitude bending and torsion loading where only the turning points in the time history are analysed (Table A1). Instead, for nonproportional loading all data points in the time history should be checked.